This project has received funding from the European Union's Seventh Programme for research, technological development and demonstration under grant agreement No [308417]".

New Directions in Seismic Hazard Assessment through Focused Earth Observation in the Marmara Supersite

Grant Agreement Number: 308417
co-funded by the European Commission within the Seventh Framework Programme
THEME [ENV.2012.6.4-2]
[Long-term monitoring experiment in geologically active regions of Europe prone to natural hazards: the Supersite concept]

D5.5 Ground motion simulation tools calibrated for the Marmara area and synthetic PGV maps

Project Start Date	1 November 2012
Project Duration	36 months
Project Coordinator /Organization	Nurcan Meral Özel / KOERI
Work Package Number	5
Deliverable Name/ Number	5.5 Ground motion simulation tools calibrated for the Marmara area and synthetic PGV maps
Due Date Of Deliverable	31 October 2014
Actual Submission Date	22 December 2014
Organization/Author (s)	Hideo Aochi, Thomas Ulrich (BRGM, France) Aybige Akinci (INGV, Italy)

Dissemination Level		
PU	Public	
PP	Restricted to other programme participants (including the Commission)	
RE	Restricted to a group specified by the consortium (including the Commission)	
CO	Confidential, only for members of the consortium (including the Commission)	

TABLE OF CONTENTS

1.Introduction

In the regions where the seismic potential in the near future is highly recognized, it is crucial to estimate quantitatively the ground motions for the expected earthquake scenarios (deterministic approach). Istanbul and its surrounding areas are warned for the future high seismic risk in the Euro-Mediterranean region (Barka et al., 2002), especially pronounced after the 1999 Izmit and Duzce earthquakes. The ground motion simulations in this region have been carried out by various researchers (Pulido et al., 2004; Sesetyan, 2007; Sørensen et al., 2007). All of them suppose a scenario earthquake of magnitude over 7 along the main trace of the North Anatolian fault, running along the north side of the Sea of Marmara (Le Pichon et al., 2003; Armijo et al., 2005). This scenario setting is consistent with the probabilistic hazard assessment and employed early warning target (Erdik et al., 2004; Sesetyan et al., 2007).

Many seismological efforts have taken place to improve the quantitative seismic hazard assessment. The fundamental question for this area and any other cases is that the probable rupture scenarios of the target earthquake are uncertain, even if a seismic gap is relatively well identified. This is a critical problem in ground motion estimation. Deterministic method of earthquake scenario generation has been proposed and used widely for the engineering purposes (e.g. Irikura and Miyake, 2011). Or stochastic parameter distribution has become useful, as often known as pseudo-dynamic approaches propose how to provide them in practical use (e.g. Song et al., 2014). In this study, we aim to introduce the dynamically simulated earthquake scenarios with weighting function in the deterministic ground motion simulations. Each simulation provides the estimation of the particular ground motion. Assembling different simulations will allow us to discuss statistically the probability and the variation of ground motion at selected sites.

2 Method and Models

2.1 Finite difference method for low frequency simulation

We carry out the 3D simulations of the seismic wave propagation in an elastic half-space using a finite difference method (FDM), based on the staggered grids with forth-order in space and second-order in time (Aochi and Madariaga, 2003). Our physical dimension is 200 km (EW) by 120 km (NS) by 40 km (depth) covering the entire Sea of Marmara and Istanbul (Figure 1). The model volume is surrounded by the absorbing boundary zones (Collino and Tsogka, 2001; Komatitsch and Martin, 2007). We adopt the 3D structure model by the recent OBS tomography (Bayrakci et al., 2013) by completing the regional 1D model (Karabulut, pers. comm.) shown in Table 1. This could be the best combination at this time (year 2014). The 3D structure model of Bayrakci et al. (2013) clearly shows the large basin structure under the Sea of Marmara up to a depth of 12 km. However their tomography is

only for the P-wave velocity (V_p) so that we suppose the S-wave velocity (V_s) as $V_s = V_p / \sqrt{3}$, and the material density

$$\rho(g/m^3) = (-0.045V_s^2 + 0.432V + 1.711) \times 1000 \qquad (1)$$

where V_s is given in km/s. The Sea of Marmara is taken into account by fixing the P- and S-wave velocities at 1500 m/s and 0 m/s. In addition to the seismic stations, other receiver points have been distributed every 3 km on the ground surface (depth = 0 km or on the ocean bottom). To take fully advantage of the available computing resources, we use both codes with CPU (Aochi and Madariaga, 2003; Dupros et al., 2008) and GPU(-CPU) parallelization (Michéa and Komatitsch, 2010). In the following simulations, we basically use a spatial grid size of 250 m, for aiming at the liable frequency context up to 0.5 Hz. However, for demonstrating the efficiency of GPU calculation, we first test a grid size of 500 m, namely about 10 millions grid numbers in total, which can be stored (about 930 Mbytes) on a single GPU memory in the institute (graphic card Nvidia Quadro K4000). This takes 600 seconds for 6000 time steps, while CPU calculation needs 1800 seconds on 48 cores (Intel AMD Abu Dhabi). This test confirms the efficiency of GPU calculation, initially reported by Michéa and Komatitsch (2010). Our GPU code can also run on multiple GPU (MPI parallelization), which enables faster computations and larger models. The multiple GPU calculations still show good performances. For a grid of 250 m, about 70 millions grids, it takes 3700 seconds for 12000 steps on 2 nodes (2 GPU graphic cards), while a CPU calculation on 192 cores requires 7200 seconds.

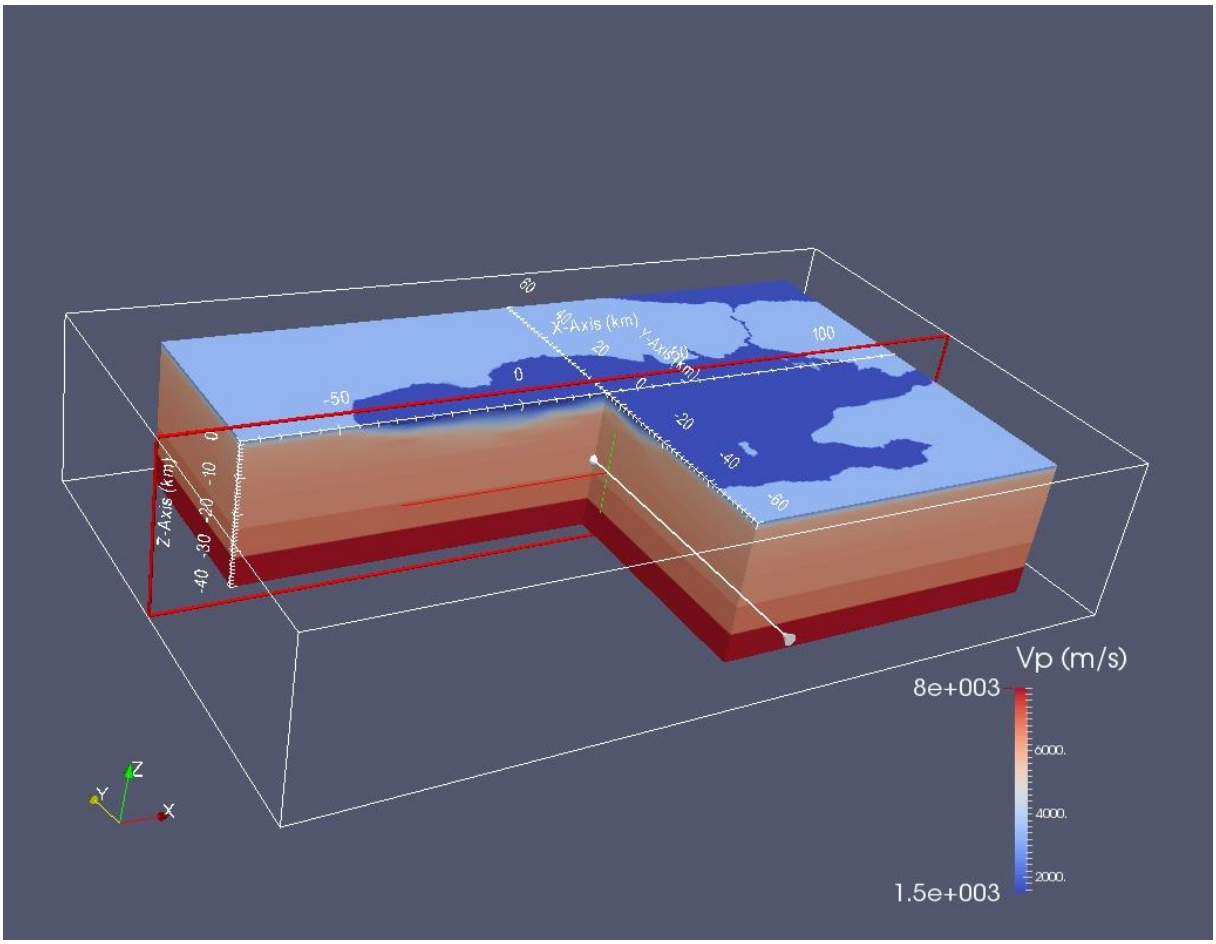

Figure 1: 3D view on the target region around the Sea of Marmara. The color indicates the P-wave velocity (Vp). The dark blue corresponds to the water layer (Vp = 1500 m/s).

Table 1: 1D structure model (Karabulut pers. comm..), combined with the 3D model of (Bayakci et al., 2013).

Top layer depth	rho	Vp	Vs
km	kg/m^3	m/s	m/s
1	2150	2.25	1.10
-1	2700	5.70	3.20
-6	2750	6.10	3.60
-20	2800	6.80	3.85
-33	2850	8.00	4.55

2.2 STOCHASTIC METHOD FOR BROADBAND GROUND MOTION SIMULATION

We used a stochastic approach to compute acceleration time series for direct S-wave field at bedrock sites (EXSIM; Boore 2009). The methodology is able to capture the complexity of near-source ground motion even when input data regarding earthquake source, propagation medium, and site characteristics are of a very schematic nature. Moreover, it allows using different rupture models (slip distribution, hypocenter position, rupture speed, stress drop, etc.) on the selected fault. The model parameters have been previously calibrated and the methods have been then demonstrated assuming different rupture scenarios in the Sea of Marmara for generating the PGA (Peak Ground Acceleration) map (periodic report of month 18). In this study, we plan to use the same earthquake models (rupture dimension and slip distribution) as the deterministic simulation presented in the above section.

2.3 SOURCE MODELS

We introduce the earthquake scenarios dynamically simulated on the non-planar fault system of the North Anatolian fault (Aochi and Ulrich, 2014). Each scenario provides the rupture history along the non-planar fault structure (seismic moment release rate at every discretized point). Practically, this is implemented using many source points (e.g. Aochi and Madariaga, 2003). The rupture are simulated for three different fault geometry models, three accumulated stress levels and three different hypocenter positions, namely for 27 scenarios in total (Table 2). A probability (between 0.5% and 7.5%) related to the likelihood of the earthquake scenarios is attributed for each parameter set through a logic tree. The aim of this paper is then to analyze the ground motion scenarios with this new combination of deterministic dynamic rupture scenarios and probabilistic parameter sets.

Table 2: Resultant moment magnitudes of the 27 earthquake scenarios dynamically simulated by Aochi and Ulrich (2014). Each parameter is given a probability according to the logic tree, based on the three levels: (1) fault geometry model, (2) accumulated stress level, (3) hypocenter location. The detail of each model parameters is given in Aochi and Ulrich (2014).The parameter T is the ratio of initial stress with respect to the dynamic strength drop on the plane optimal to the external principal stress field.

(a) Complex fault geometry model (45%)

Hypocenter position	Accumulated stress level		
	Extremely high	High	Sufficient
	T = 0.97 (15%)	T = 0.75 (35%)	T = 0.66 (50%)
Center (33.3%)	7.45	7.27	7.104
East (33.3%)	7.45	7.26	5.98
West (33.3%)	7.45	5.87	5.73

(b) Intermediate fault geometry model (45%)

	T = 0.97	T = 0.75	T = 0.66
Center	7.49	7.29	7.04
East	7.46	7.29	7.19
West	5.76	5.59	5.49

(c) Smooth fault geometry model (10%)

	T = 0.97	T = 0.75	T = 0.66
Center	7.56	7.41	5.79
East	7.53	7.41	5.98
West	7.56	5.96	5.83

3 Results

3.1 PGV maps from finite difference simulation

Each simulation provides the time histories at 2851 receiver points. A uniform grid of regularly distributed receivers (step 3 km), completed by the actual receivers of the observation network, is considered to generate the PGV (Peak Ground Velocity) map. In the sea area, the receivers are set at the uppermost position of rock material, namely at the Sea bottom. In the land part, the receivers are set to be zero height, as the ground surface is considered flat. Figure 2 shows the PGV maps corresponding to the nine cases based on the LP fault geometry model. The three right-bottom panels correspond to earthquakes of magnitude smaller than 6. The large PGV areas (i.e. green to yellow) are limited to the epicenter position and to areas extending in the EW and NS directions in accordance with

the radiation pattern of the S-wave. For the other six cases of large earthquakes (Mw > 7), it is observed that the very large PGV areas (i.e. red) extend not only around the causal earthquake fault but also much further away. In particular, for the cases where the stress accumulated was extremely high, we observe that the red zone extends linearly along the fault trace. This is a characteristic feature of super-shear rupture propagations (Dunham and Bhat, 2008).

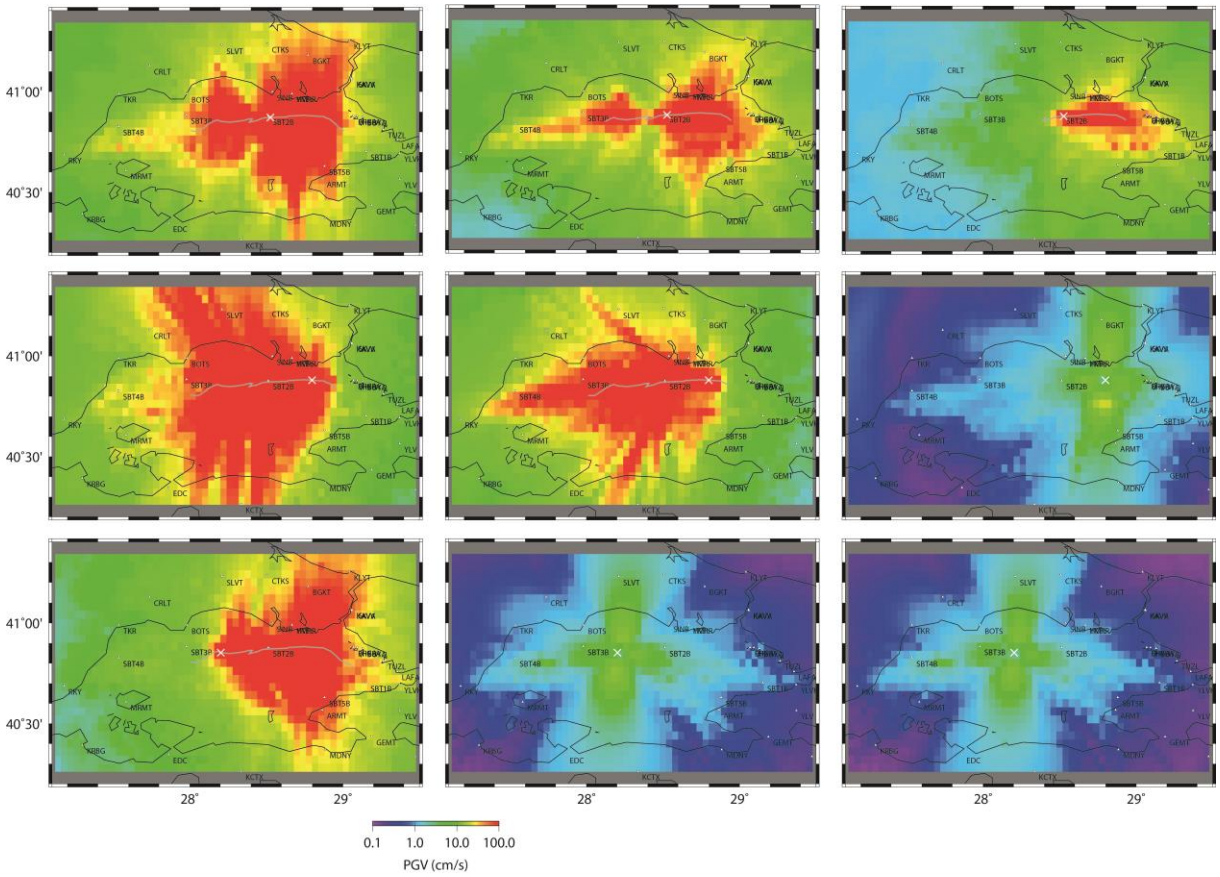

Figure 2: PGV (peak ground velocity) map for three components from each ground motion simulation. All the nine cases shown here are based on the fault geometry model LP. From left to right, the supposed stress level in generating the earthquake rupture scenario is respectively extremely high, high and sufficient. From top to bottom, the hypocenter position, denoted by a white cross, is located respectively in the central, eastern and western part of the fault. The ruptured fault trace is shown by a grey line. The time series of ground motions are processed by a 0.5 Hz low-pass filter.

3.2 Statistical analyses on ground motion estimation

Let us choose a receiver in the center of Istanbul (41.0425°N, 28.9968°E). At this location, Vs = 1780 m/s on the ground surface of our structural model. Each earthquake scenario has been attributed a probability ranging from 0.5 to 7.5 %. We can then estimate the expected ground motion level using these probabilities. Figure 3 shows an analysis of the PGV values of the 27 simulations. The PGV is smaller than 0.1 m/s for all the simulated earthquakes of magnitude smaller than 6, while values up to 1.4 m/s are observed for the events of

magnitude larger than 7. The possibility of an extremely large PGV exceeding 1 m/s is limited, but not denied, though more probably the PGV would be smaller than 0.4 m/s.

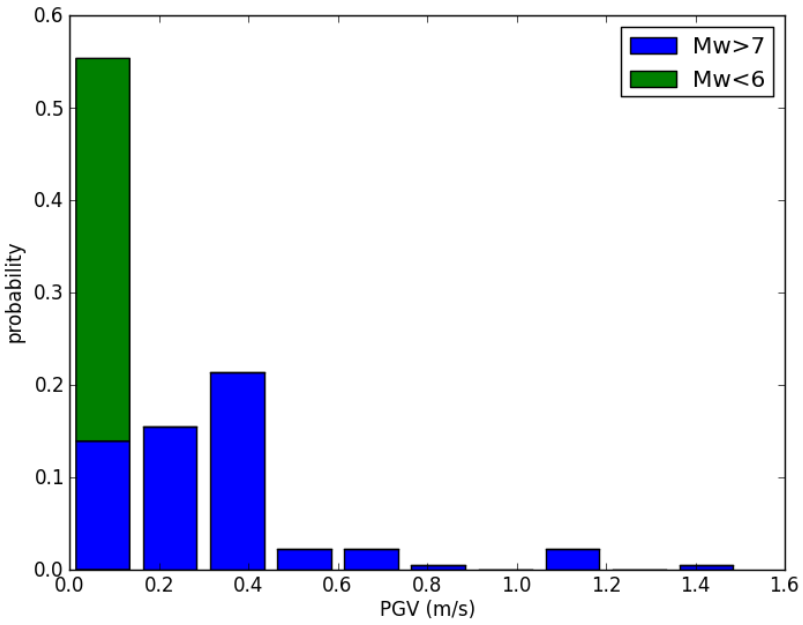

Figure 3: Probability of observation of a given PGV at the point (41.0425°N, 28.9968°E).

3.3 PGV map from stochastic simulation

For the earthquake scenarios, selection of the possible earthquake source locations, its geometrical, kinematical structure and parameters and the starting point of fault rupture are very important issues. In this study, we presented the strong-ground-motion simulations from selected earthquake scenarios using a stochastic finite-fault model with a dynamic corner frequency approach Motazedian and Atkinson (2005). In order to produce the high frequency ground motions in the region we have chosen one of the nine cases of the LP fault geometry model (the scenario earthquake ruptures) given by the BRGM working group during the first semester of the project. We selected a model called LP calculated using a sufficient accumulated stress, T = 0.66, M_w=7.04 and given by a one central slip asperity distribution model (figure 4a and b; see previous section for details) for our stochastic PGA and PGV simulations both in time and frequency domains to be used for high frequency part of the broadband seismograms.

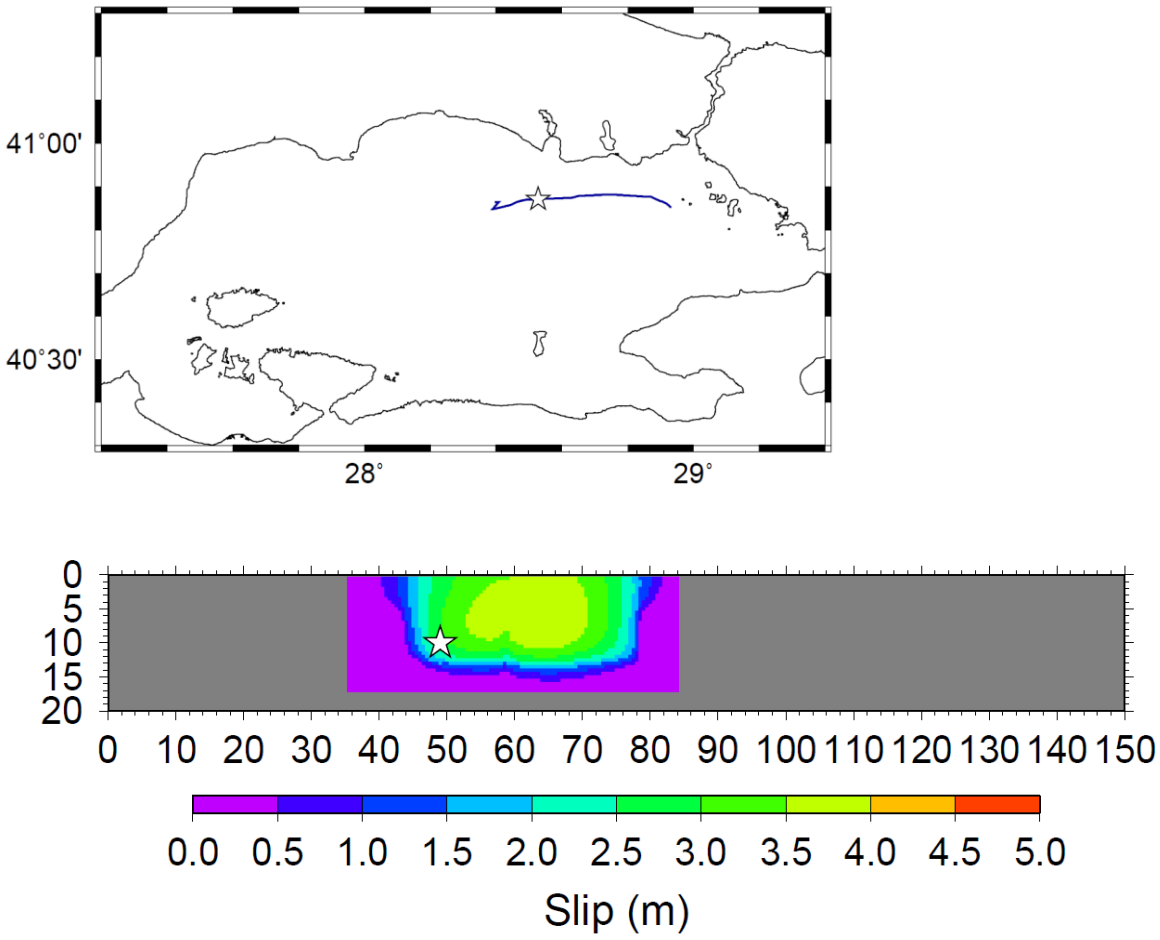

***Figure 4** and **b.** Surface rupture and slip asperity distribution along the selected fault.*

The stochastic method based on a dynamic corner frequency approach needs some definitions of the spectral parameters, such as stress drop, geometrical spreading, quality factor Q and diminution parameter κ (taken from **Error! Reference source not found.**Akinci *et al.* 2006) and the selected fault, including focal depth and source mechanisms, are listed in **Table 3** (taken from dynamic rupture modeling).

***Table 3.** Fault model parameters, Length, strike and dip of model fault plane are based on the dynamic rupture modeling.*

	LP M7.04 Fault
East end	40.85N-28.93E
West end	40.87N-28.40E
L (km)	50
W (km)	20
LxW rupture	50x20 km^2
M*	7.04
Strike(deg)	88
Dip (deg)	90
Focal mechanism	Right-lateral strike slip

For selected fault model the synthetics were computed at 180 sites for this rupture scenario, obtained by the combination of slip model (**Figure 4ab**). The ground motion parameters computed at bedrock sites are displayed with contour maps for PGA and PGV. The largest peak ground value for the selected scenario reach 1.0 g for PGA and 80-90 cm/sec for PGV (see **Figure 5a** and **b**). The position of the maximum shaking area is located close to the southwestern coast of the European side of Istanbul close to the Bakirkoy and Avclar districts.

Secondly we compared those simulated ground acceleration and velocity values with those calculated using two different slip distributions; uniform and random weighted slip distributions on the same fault. In both cases the maxima is related to the directivity effects (rupture process on extended fault). The computed values clearly depend on the position of nucleation point, whereas the slip model modifies the maxima distribution at the sites close to the fault and according to the asperity location. The maximum PGA and PGV is lower for the uniform and random slip distribution models with right lateral nucleation point (**Figure 6ab** and **7ab**), varying from about 0.6 g and 40-45 cm/sec for uniform slip model and 0.7 g and 55-60 cm/sec for random slip model, respectively. The maximum value is obtained for the LP slip distribution model where the slip asperity is located in the middle of the fault that could generate PGA values up to 1 g and 90 cm/sec.

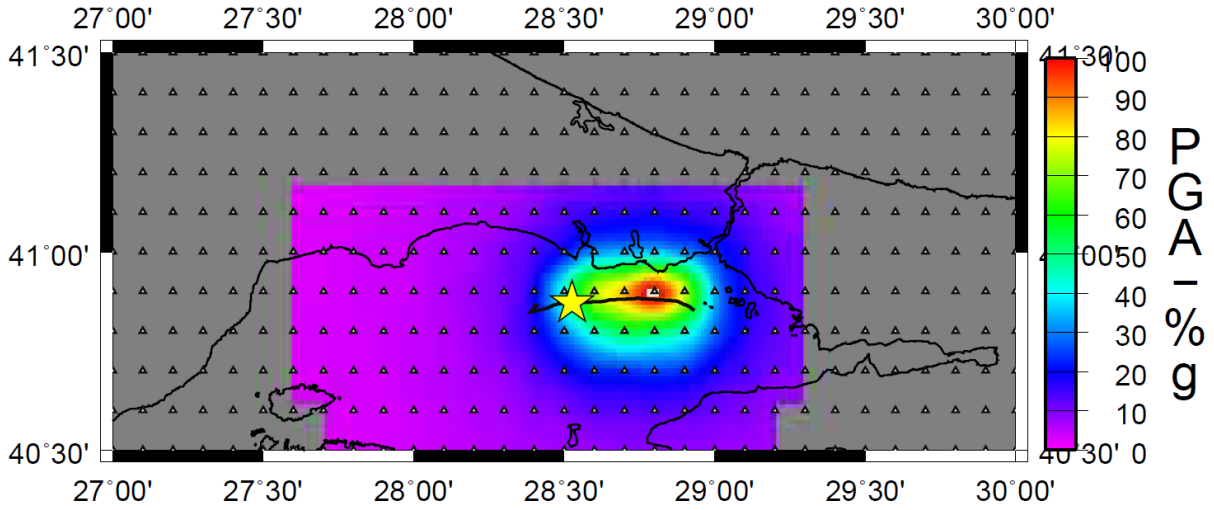

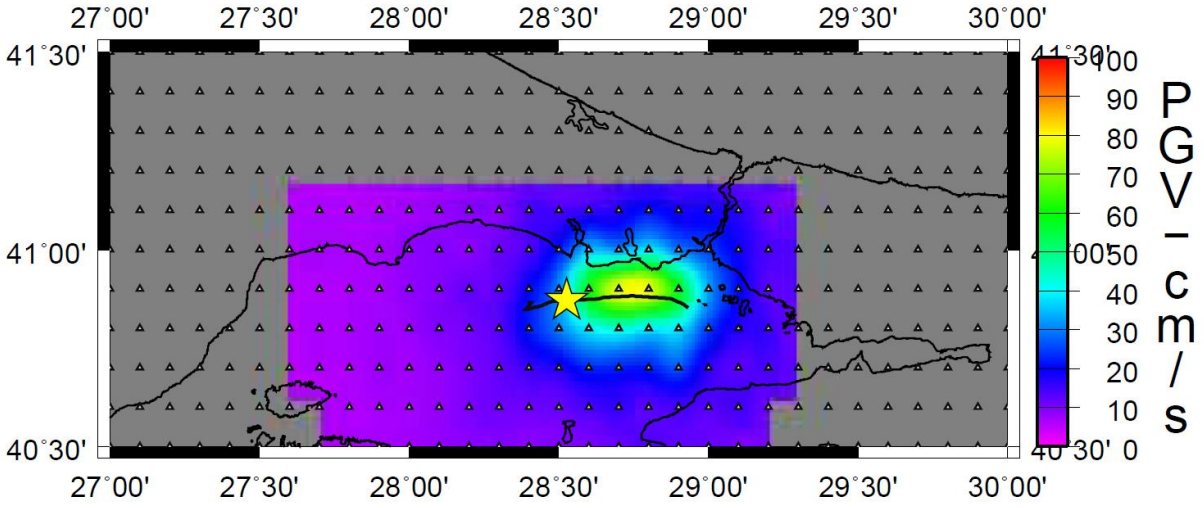

Figure 5a** and **b PGA and PGV maps for rupture model with slip model LP (one central asperity see figure 5 b) and left nucleation point. Position of receivers is given by triangles.

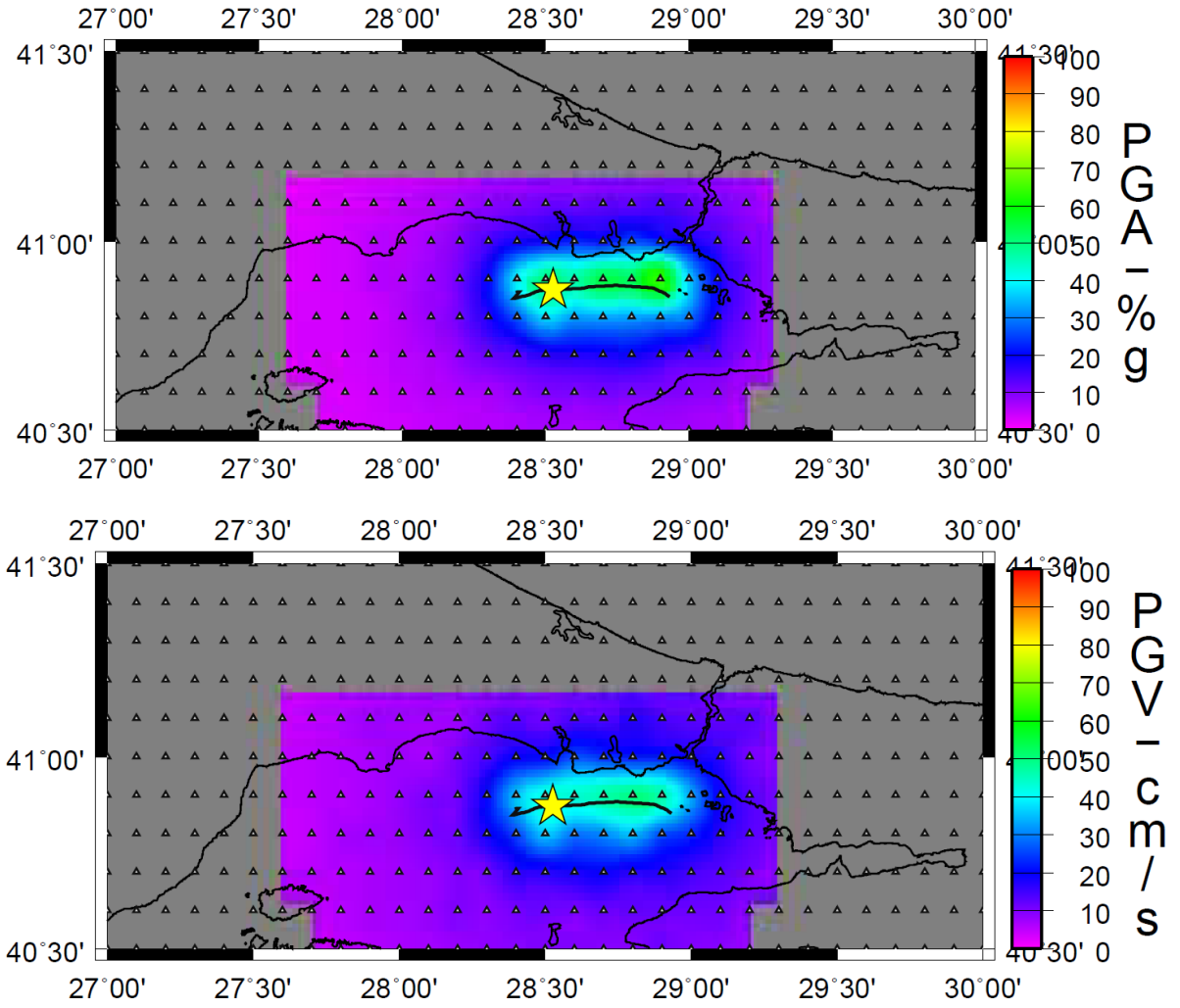

Figure 6a** and **b PGA and PGV maps for rupture model with random slip distribution and left side nucleation point. Position of receivers is given by triangles.

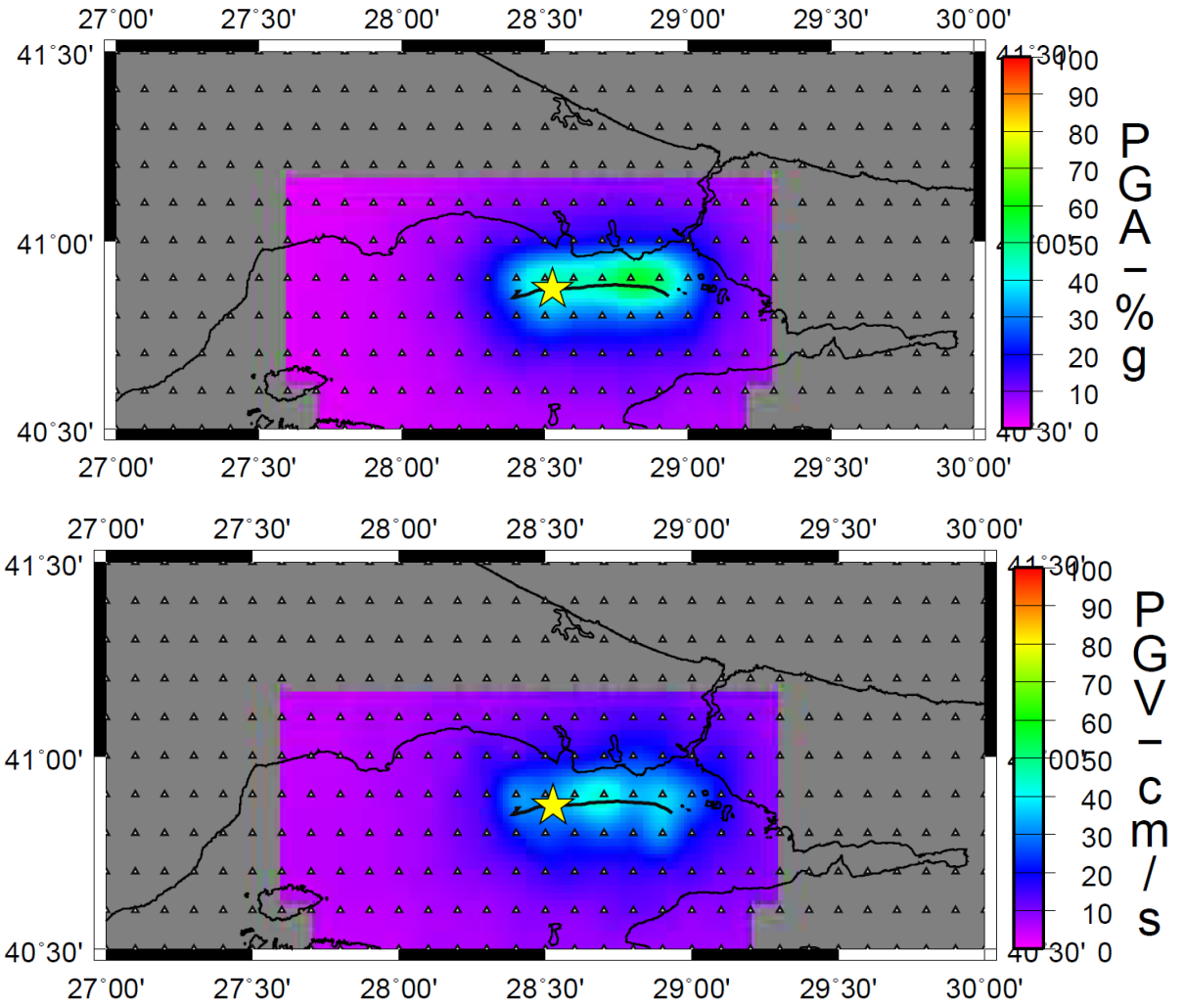

Figure 7a** and **b PGA and PGV maps for rupture model with uniform slip distribution model and left nucleation point. Position of receivers is given by triangles.

4 Perspective and Conclusion

In this report, we demonstrated our methodology of ground motion simulation adjusted for the Sea of Marmara. In particular, we assembled the available data about the structure models for constructing heterogeneous medium and adopt the earthquake scenarios dynamically and stochastically simulated with weighing functions. This provides the regional PGV map for each simulation and then allows analyzing statistically the ground motion estimations. It will be still necessary to calibrate better the model parameters through the tests of known moderate earthquakes.

References

Akinci, A., L. Malagnini, R. B. Herrmann, R. Gok, and M. Sorensen, 2006. Ground Motion Scaling in the Marmara Region, Turkey. ***Geophysical Journal International,*** *166, p. 635–651.*

Ansal, A., Akinci, A., Cultrera, G., Erdik, M., Pessina, V., Tuzce, G. and Ameri, G., 2009. Loss estimation in Istanbul based on deterministic earthquake scenarios in the Marmara Sea region, Turkey. *Soil Dynamics and Earth. Eng.*

Aochi, H., Durand, V., Douglas, J., 2011, Influence of super-shear earthquake rupture models on simulated near-source groud motion from the 1999 Izmit, Turkey, earthquake, Bull. Seism. Soc. Am., 101, 726-741.

Aochi, H. and R. Madariaga (2003), The 1999 Izmit, Turkey, earthquake: Non-planar fault structure, dynamic rupture process and strong ground motion, Bull. Seism. Soc. Am., 93, 1249-1266, doi:10.1785/0120020167.

Aochi, H. and T. Ulrich, 2014, A probable earthquake scenario near Istanbul determined from dynamic simulations, in revision, Bull. Seism. Soc. Am.

Barka, A., H. S. Akyüz, E. Altunel, G. Sunal, Z. Cakir, A. Dikbas, B. Yerli, R. Armijo, B. Meyer, J. B. de Chabalier, T. Rockwell, J. R. Dolan, R. Hartleb, T. Dawson, S. Christofferson, A. Tucker, T. Fumal, R. Langridge, H. Stenner, W. Lettis, J. Bachhuber, and W. Page (2002). The surface rupture and slip distribution of the August 17, 1999 Izmit earthquake, M 7.4, North Anatolian Fault, Bull. Seismol. Soc. Am. 92, 43–60.

Bayrakci, G., M. Ligle, A. Bécel, A. Hirn, T. Taymaz, S. Yolsal-Çevikbilen and SEISMARMARA team (2013), 3-D sediment-basement tomography of the Northern Marmara trough by a dense OBS network at the nodes of a gri of controlled source profiles along the North Anatolian fault, Geophys. J. Int. doi:20.1093/gji/ggt211.

Boore, D. M. (2009). Comparing stochastic point-source and finite-source ground-motion simulations: SMSIM and EXSIM, *Bull. Seism. Soc. Am.* **99**, 3202-3216.

Collino, F., and C. Tsogka (2001). Application of the perfectly matched absorbing layer model to the linear elastodynamic problem in anisotropic heterogeneous media, Geophysics 66, 294–307.

Dupros, F., H. Aochi, A. Ducellier, D. Komatitsch, and J. Roman (2008). Exploiting intensive multithreading for efficient simulation of seismic wave propagation, in the Proc. of the 11th Int. Conf. on Computational Science and Engineering, 253–260, San Paulo, Brazil, June 2008.

Dunham, S. and H. S. Bhat (2008). Attenuation of radiated ground motion and stresses from three-dimensional supershear ruptures, J. Geophys. Res., 113, doi:1029/2007JB005182.

Erdik, M., M. Demircioğlu, K. Sesetyan, E. Durukal, B. Siyahi (2004), Earthquake hazard in Marmara region, Turkey, Soil Dyn. Earthq. Eng., 24, 605-631.

Irikura, K. and H. Miyake (2011). Recipe for predicting strong ground motion from crustal earthquake scenarios, Pure Appl. Geophys. 168:85-104, doi:10.1007/s00024-010-0150-9.

Komatitsch, D., and R. Martin (2007). An unsplit convolutional perfectly matched layer improved at grazing incidence for the seismic wave equation, Geophysics 72, no. 5, SM155–SM167.

Michea, D., and D. Komatitsch (2010). Accelerating a 3D finite-difference wave propagation code using GPU graphics card, Geophys. J. Int. 182, 389–402.

Motazedian, D., and G. M. Atkinson (2005). Stochastic finite-fault modeling based on a dynamic corner frequency, Bull. Seismol. Soc. Am. 95,

995–1010. Pulido, N., A. Ojeda, K. Atakan, T. Kubo (2004), Strong ground motion esimatio in the Marmara Sea region (Turkey) based on a scenario earthquake, Tectonphys., 391, 357-374.

Song, S. G., L. A. Dalguer, P. M. Mai (2014). Pseudo-dynamic modellin with 1-point and 2-point statistics of earthquake source parameters, Geophys. J. Int., 196, 1770-1786, doi:10.1093/gji/ggt479.

Sørensen, M. B., N. Pulido,and K. Atakan (2007), Sensitivity of ground-motion simulations to earthquake source parameters: A case study for Istanbul, Turkey, Bull. Seism. Soc. Am., 97, 881-900, doi: 10.1785/0120060044.

Sesetyan, K. (2007) Characterization of response spectra for near field conditions by earthquake ground motion simulation, PhD thesis, University Paris-Sud, Orsay, France.

Sesetyan, K., C. Zulfikar, M. Demircioglu, U. Hancilar, Y. Kamer and M. Erdik (2011), Istanbul earthquake rapid response system: Methods and practices, Soil Dyn. Earthq. Eng., 31, 170-180.